

Characterization and Electrochemical Properties of $\text{LiNi}_{0.5}\text{Mn}_{1.5}\text{O}_4$ Prepared by a Carbonate Co-Precipitation Method

Yi-Jie Gu^{1,2,*}, Qing-Feng Zang¹, Hong-Quan Liu¹, Jian-Xu Ding¹, Yan-Ming Wang¹, Hai-Feng Wang², Jun Zhang¹, Wen-Ge Wei¹

¹ College of Materials Science and Engineering, Shandong University of Science and Technology, Qingdao 266510, China

² Rizhao Huaxuan New Energy Co., Ltd., Rizhao 276826, China

*E-mail: guyijie@sdust.edu.cn

Received: 4 September 2014 / Accepted: 15 October 2014 / Published: 28 October 2014

$\text{LiNi}_{0.5}\text{Mn}_{1.5}\text{O}_4$ is synthesized using $\text{Ni}_{0.5}\text{Mn}_{1.5}(\text{CO}_3)_2$, which is prepared by a carbonate co-precipitation method at pH values of 7.5, 7.8, 8.0 and 8.3. The Rietveld refinements reveal Li and Ni site substitution in $\text{LiNi}_{0.5}\text{Mn}_{1.5}\text{O}_4$. The preparation pH is found to affect Li and Ni site substitution in $\text{LiNi}_{0.5}\text{Mn}_{1.5}\text{O}_4$. For the compound prepared at a pH of 8.3, high capacity and a high Li ion diffusion coefficient are achieved.

Keywords: Lithium and Nickel site substitution; cathode material; electrochemical properties

1. INTRODUCTION

Lithium-ion secondary batteries have received much recent attention. Lithium-ion batteries have become an important power source for portable electronic devices such as laptop computers, cell phones, hybrid electrical vehicles (HEV) and electrical vehicles (EV) because of their high output [1-3]. Because the electrode material is the basic element of any battery, many studies have focused on the development of cathode materials to achieve high output voltage, high specific energy, small self-discharge, no memory effects, and good safety features [4, 5]. It is commonly believed that electrochemical systems with excellent power properties can be achieved by a low amount of Ni substitution at the Li site in LiMO_2 (M = Ni, Co and Mn). Ni substitution at the Li site was found to be the best theory to determine and control the electrochemical properties of LiMO_2 layered structures.

LiMn_2O_4 spinel has been studied widely owing to its low cost, environmental friendliness, and safety performance [6]. However, stoichiometric LiMn_2O_4 has been shown to exhibit poor cycling

behavior. An approach used to improve the cycling behavior is the substitution of Mn with transition metals to produce $\text{LiM}_x\text{Mn}_{2-x}\text{O}_4$ ($\text{M}=\text{Co}, \text{Cr}, \text{Ni}, \text{Fe}, \text{etc.}$)[7]. Ni substitution overcomes the drawbacks of lattice distortion and also increases the voltage plateaus at around 4.7 V [7]. It is well known that $\text{LiNi}_{0.5}\text{Mn}_{1.5}\text{O}_4$ has excellent cycling behavior and high capacity. Because of the above-mentioned merits, $\text{LiNi}_{0.5}\text{Mn}_{1.5}\text{O}_4$ is regarded as a promising 5-V class cathode material for high-power EV applications.

Here, we show that $\text{LiNi}_{0.5}\text{Mn}_{1.5}\text{O}_4$, which obtains high energy density by carbonate co-precipitation. There is a direct relationship between the extent of Ni substitution of the Li sites and the preparation pH. The effect of preparation pH on the physical and electrochemical properties is discussed.

2. EXPERIMENTAL

A $\text{Ni}_{0.5}\text{Mn}_{1.5}(\text{CO}_3)_2$ precursor was first prepared by co-precipitation in a continuous stirred tank reactor (CSTR). Nickel sulfate hexahydrate ($\text{NiSO}_4 \cdot 6\text{H}_2\text{O}$), manganese sulfate monohydrate ($\text{MnSO}_4 \cdot \text{H}_2\text{O}$), natronite (Na_2CO_3) and ammonium hydroxide ($\text{NH}_3 \cdot \text{H}_2\text{O}$) were used as starting materials. One hundred ml of a 1-M mixed acid solution of NiSO_4 and MnSO_4 ($\text{Ni}:\text{Mn} = 1:3$ molar ratio) was fed into the reactor using a peristaltic pump. The pH was well controlled using a pH meter, and the target pH values were 7.5, 7.8, 8.0 or 8.3. The co-precipitation temperature was set at 55 °C and the agitation rate was 800 r/min. The obtained particles were calcined at 600 °C for 5 h and the carbonate decomposed into an oxide. The collected precursor was then mixed with a stoichiometric amount of Li_2CO_3 and placed in a crucible, and then calcined at 850 °C for 10 h in a muffle furnace.

The structure of the obtained $\text{LiNi}_{0.5}\text{Mn}_{1.5}\text{O}_4$ was characterized by X-ray powder diffraction (XRD, D/Max2500PC, Japan) with a Cu anticathode, $\text{K}\alpha$ radiation, graphite monochromator, 30-kV tube voltage, 100-mA tube current, and a step size of 0.02° in the range of $10\text{--}120^\circ$. The morphology and microstructure of the samples were obtained by scanning electron microscopy (SEM). A tap density meter (FZS4-4B) was used to determine the tap density. The chemical compositions of the synthesized materials were determined using an inductively coupled plasma spectrometer (ICP: Agilent7500a). The ICP analysis reveals that the metal compositions of the $\text{LiNi}_{0.5}\text{Mn}_{1.5}\text{O}_4$ at preparation pH values of 7.5, 7.8, 8.0 and 8.3 are similar to the starting composition.

All electrochemical measurements were performed on materials in the form of a CR2016 type coin cell with metallic lithium as the reference anode. The as-prepared $\text{LiNi}_{0.5}\text{Mn}_{1.5}\text{O}_4$, carbon black, and polyvinylidene fluoride (PVDF) were mixed in a weight ratio of 8:1:1 in the presence of a small amount of N-methyl-2-pyrrolidone (NMP). The slurry was coated onto aluminum foil and then dried in a vacuum oven at 120 °C for 12 h. The electrolyte was a 1 M LiPF_6 solution in a mixture of ethylene carbonate (EC)/dimethyl carbonate (DMC) (EC/DMC, volume ratio 1:1). A Cellgard2400 membrane was used as an electrode separator. Charge/discharge tests were carried out in a voltage range of 3.5–4.9 V with a LAND-CT2001A battery test system. Electrochemical impedance spectroscopy (EIS) measurements were obtained using a Zahner Elektrik IM6 impedance analyzer over the frequency range from 100 kHz to 10 mHz with an amplitude of 10 mv.

3. RESULTS

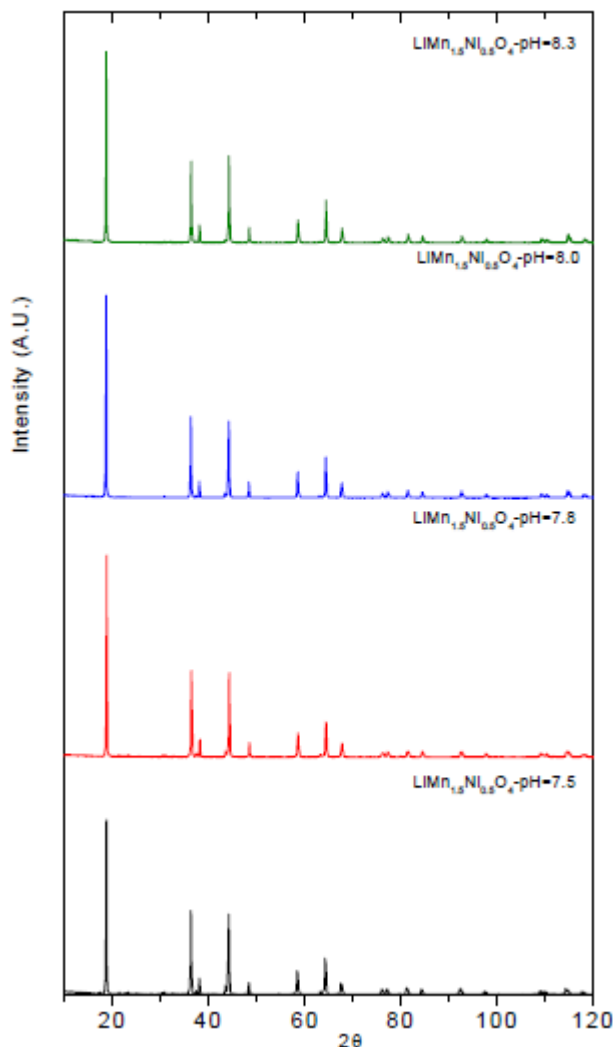


Figure 1. XRD patterns of the samples synthesized at different pH values.

Fig. 1 shows an XRD pattern of as-prepared $\text{LiNi}_{0.5}\text{Mn}_{1.5}\text{O}_4$ at preparation pH values of 7.5, 7.8, 8.0 and 8.3. All the diffraction peaks can be indexed to a well-defined spinel cubic structure (Fd-3m). The XRD patterns of the samples obtained at preparation pH values of 7.5, 7.8, 8.0 and 8.3 were refined. The X-ray diffraction data of the parent $\text{LiNi}_{0.5}\text{Mn}_{1.5}\text{O}_4$ (pH=7.5, 7.8, 8.0 and 8.3) samples were first fit to a strict three-dimensional model based on a spinel cubic structure, $[\text{Li}]_{8a}[\text{Ni}_{0.5}\text{Mn}_{1.5}]_{16d}[\text{O}_4]_{32e}$. This fit gave negative values for the atomic displacement parameter B_{Li} , indicating excess electron density in the lithium site and also cation mixing. A refinement was carried out using a model in which a fraction of the Ni^{2+} ions was allowed to be in the lithium site, $[\text{Li}_{1-z}\text{Ni}_z]_{8a}[\text{Ni}_{0.5-z}\text{Mn}_{1.5}\text{Li}_z]_{16d}[\text{O}_4]_{32e}$. In this model, only Ni^{2+} and no Mn^{4+} was allowed to replace lithium because the radius of Mn^{4+} was 0.54 Å which is smaller than the radius of Li^+ . The XRD pattern of the sample precipitated at pH 8.3 together with its refinement is shown in Fig. 2. Table 1 gives the structural parameters for $\text{LiNi}_{0.5}\text{Mn}_{1.5}\text{O}_4$ and these were obtained from a refinement of the XRD data.

A refinement of the XRD pattern of the $\text{LiMn}_{1.5}\text{Ni}_{0.5}\text{O}_4$ prepared at a pH of 7.5 led to a cationic distribution in the pristine material $[\text{Li}_{0.924}\text{Ni}_{0.076}]_{8a}[\text{Mn}_{1.5}\text{Ni}_{0.424}\text{Li}_{0.076}]_{16d}\text{O}_4$. At a $\text{LiMn}_{1.5}\text{Ni}_{0.5}\text{O}_4$ preparation pH of 7.8, the formula $\text{LiMn}_{1.5}\text{Ni}_{0.5}\text{O}_4$ described the structure $[\text{Li}_{0.952}\text{Ni}_{0.048}]_{8a}[\text{Mn}_{1.5}\text{Ni}_{0.452}\text{Li}_{0.048}]_{16d}\text{O}_4$ well. When the preparation pH was increased to 8, the occupation of Ni^{2+} ions in the lithium site was found to be 0.032. This decreased to 0.02 when the preparation pH was increased to 8.3. Therefore, the formula $\text{LiMn}_{1.5}\text{Ni}_{0.5}\text{O}_4$ may be represented as $[\text{Li}_{0.98}\text{Ni}_{0.02}]_{8a}[\text{Mn}_{1.5}\text{Ni}_{0.48}\text{Li}_{0.02}]_{16d}\text{O}_4$ according to the refined XRD data. Fig. 3 shows the variation in the occupation of Ni^{2+} ions in the lithium site as the preparation pH increases. The occupation of Ni^{2+} ions in the lithium site decreased with an increase in preparation pH.

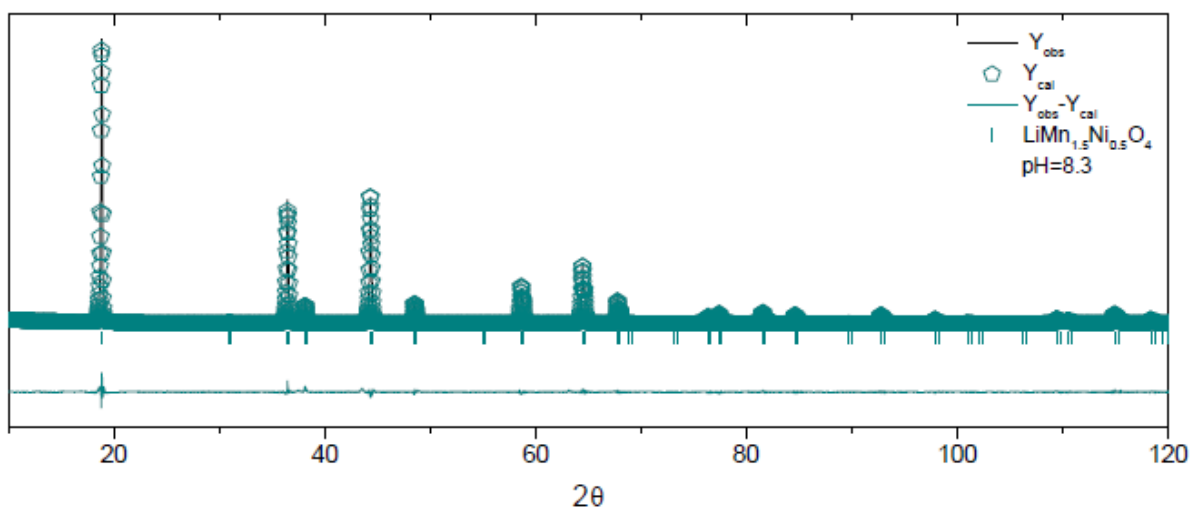


Figure 2. Comparison of the experimental and calculated XRD patterns of $\text{LiMn}_{1.5}\text{Ni}_{0.5}\text{O}_4$. Constraints: $n(\text{Li})_{8a} + n(\text{Ni})_{8a} = 1$; $n(\text{Li})_{16d} + n(\text{Ni})_{16d} + n(\text{Mn})_{16d} = 1$.

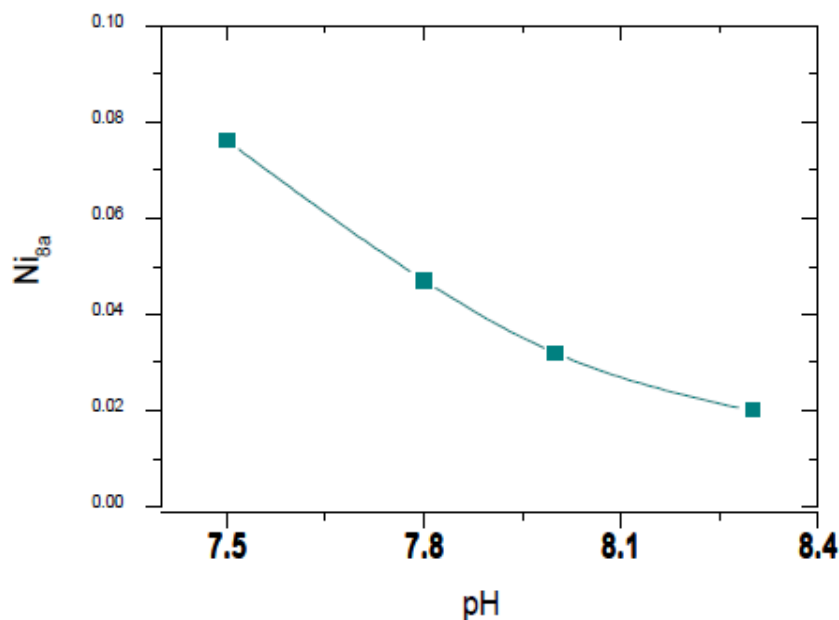


Figure 3. Variation of Ni^{2+} in the Li site of $\text{LiMn}_{1.5}\text{Ni}_{0.5}\text{O}_4$ as the pH increases.

Table 1. Structural parameters for the $\text{LiNi}_{0.5}\text{Mn}_{1.5}\text{O}_4$ compounds.

		$\text{LiMn}_{1.5}\text{Ni}_{0.5}\text{O}_4$ pH=7.5	$\text{LiMn}_{1.5}\text{Ni}_{0.5}\text{O}_4$ pH=7.8	$\text{LiMn}_{1.5}\text{Ni}_{0.5}\text{O}_4$ pH=8.0	$\text{LiMn}_{1.5}\text{Ni}_{0.5}\text{O}_4$ pH=8.3
Space group		Fd-3m	Fd-3m	Fd-3m	Fd-3m
Lattice constant					
a(Å)		8.1992(2)	8.1863(2)	8.17393(14)	8.17097(13)
Cell volume(Å ³)		551.2068	548.6091	546.1259	545.5328
Structure parameters					
R_p		9.52	9.84	8.3	8.1
R_{wp}		13.7	15.6	12.6	11.8
Li_{8a}	x	0.37500	0.37500	0.37500	0.37500
	y	0.37500	0.37500	0.37500	0.37500
	z	0.37500	0.37500	0.37500	0.37500
	Occ	0.03863(15)	0.03969(16)	0.04034(14)	0.04084(14)
	B	1.5(3)	1.3(3)	1.7(3)	1.6(3)
Ni_{8a}	x	0.37500	0.37500	0.37500	0.37500
	y	0.37500	0.37500	0.37500	0.37500
	z	0.37500	0.37500	0.37500	0.37500
	Occ	0.00304(15)	0.00198(16)	0.00133(14)	0.00083(14)
	B	1.5(3)	1.3(3)	1.7(3)	1.6(3)
Mn_{16d}	x	0	0	0	0
	y	0	0	0	0
	z	0	0	0	0
	Occ	0.06250	0.06250	0.06250	0.06250
	B	0.36(3)	0.47(3)	0.27(2)	0.215(19)
Ni_{16d}	x	0	0	0	0
	y	0	0	0	0
	z	0	0	0	0
	Occ	0.01779	0.01885	0.01950	0.02000
	B	0.36(3)	0.47(3)	0.27(2)	0.215(19)
Li_{16d}	x	0	0	0	0
	y	0	0	0	0
	z	0	0	0	0
	Occ	0.00304	0.00198	0.00133	0.00083
	B	0.36(3)	0.47(3)	0.27(2)	0.215(19)
O_{32e}	x	0.23770(17)	0.23732(18)	0.23756(15)	0.23776(15)
	y	0.23770(17)	0.23732(18)	0.23756(15)	0.23776(15)
	z	0.23770(17)	0.23732(18)	0.23756(15)	0.23776(15)
	Occ	0.16666	0.16666	0.16666	0.16666
	B	1.51(6)	1.39(7)	1.12(5)	1.07(5)

The SEM pattern of the precursor powder $\text{Ni}_{0.5}\text{Mn}_{1.5}(\text{CO}_3)_2$ is shown in Fig. 4, and an obvious double peak is present for the pH 7.8 prepared compound shown in Fig. 5. D(90) has a minimum

particle size at a preparation pH of 8.3, as shown in Fig. 6. Fig. 7 shows the effect of preparation pH on the tap density of $\text{Ni}_{0.5}\text{Mn}_{1.5}(\text{CO}_3)_2$. High tap density materials can be made at a preparation pH of 8.3.

The initial charge–discharge curves of the $\text{LiNi}_{0.5}\text{Mn}_{1.5}\text{O}_4$ synthesized at different pH values were recorded by cycling cells between 3.5 and 4.9 V at a constant current rate of 0.1 C. Fig. 8 shows that the sample had two voltage plateaus at approximately at 4.0 and 4.7 V [8, 9]. The highest initial discharge capacity of 128 mAhg^{-1} was obtained for the sample prepared at a pH of 8.3. The others were 98 mAhg^{-1} , 105 mAhg^{-1} and 104 mAhg^{-1} for preparation pH values of 7.5, 7.8 and 8.0, respectively.

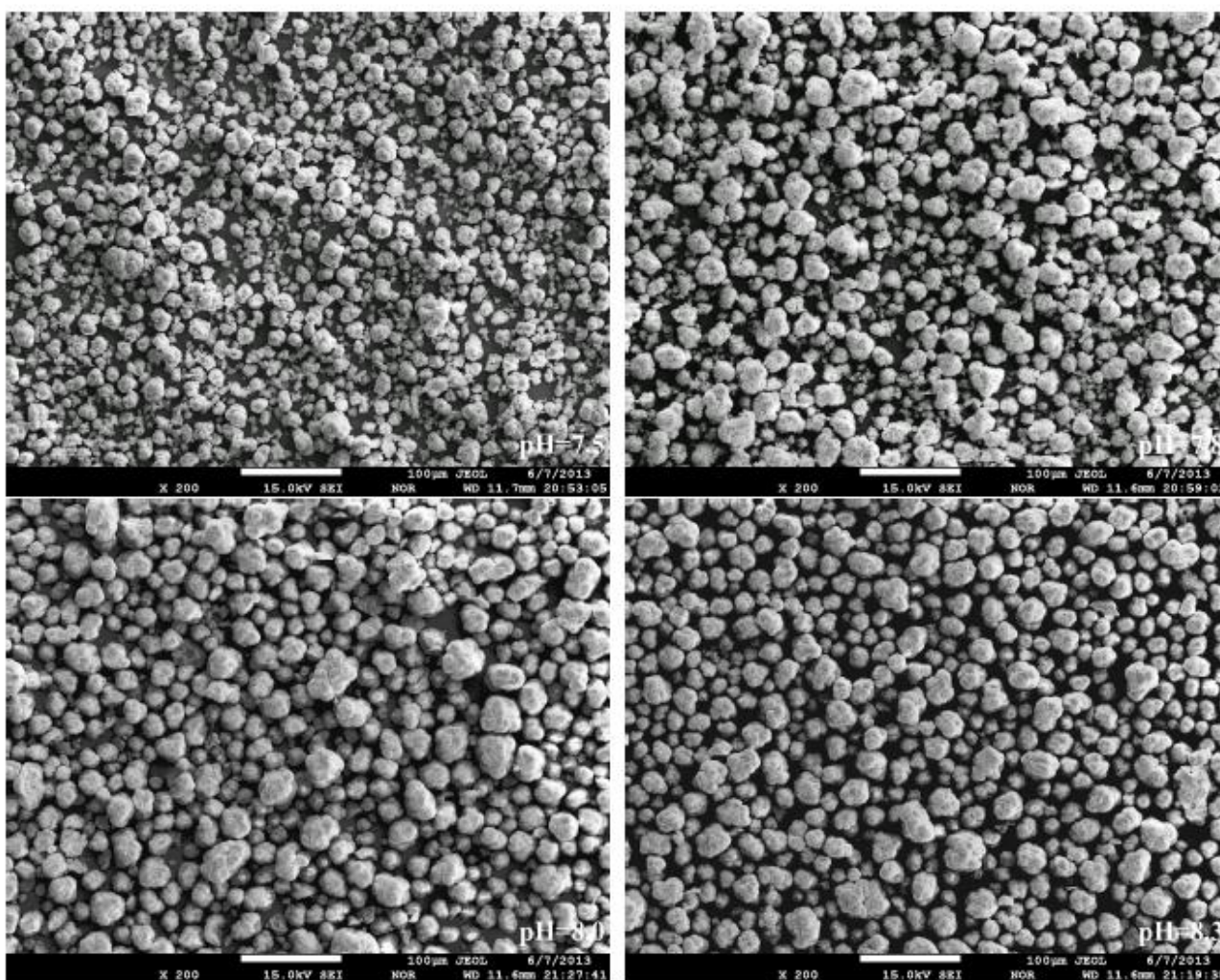


Figure 4. SEM images of the sample precursors collected at different pH value.

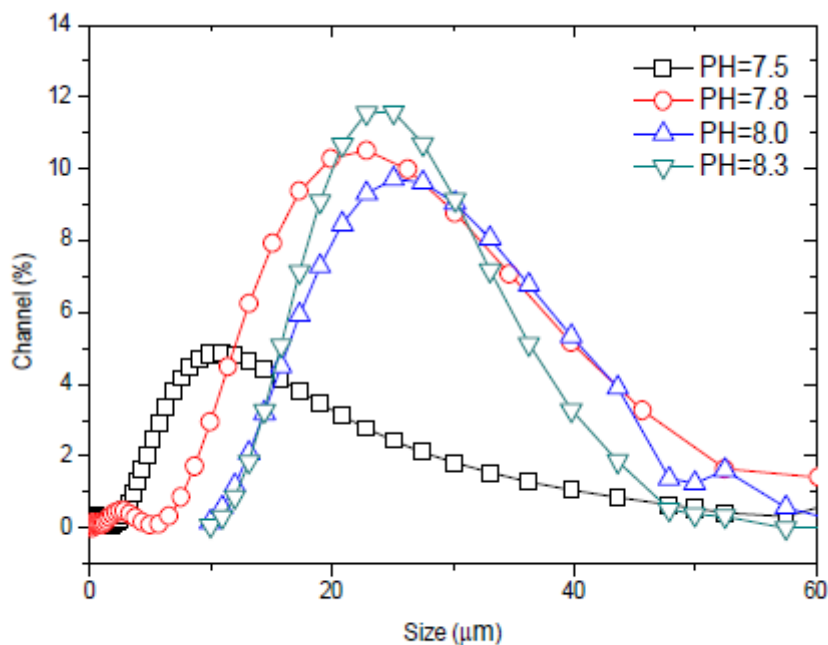


Figure 5. Particle size distribution of the precursors at different preparation pH values.

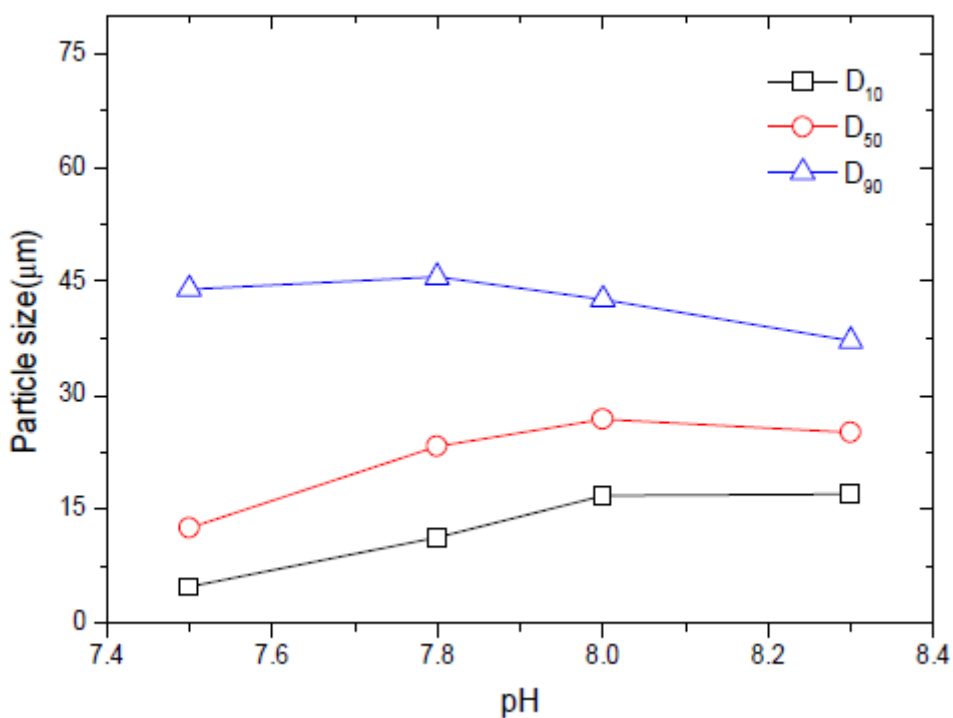


Figure 6. Average particle size (D10, D50, D90) evolution as a function of the preparation pH.

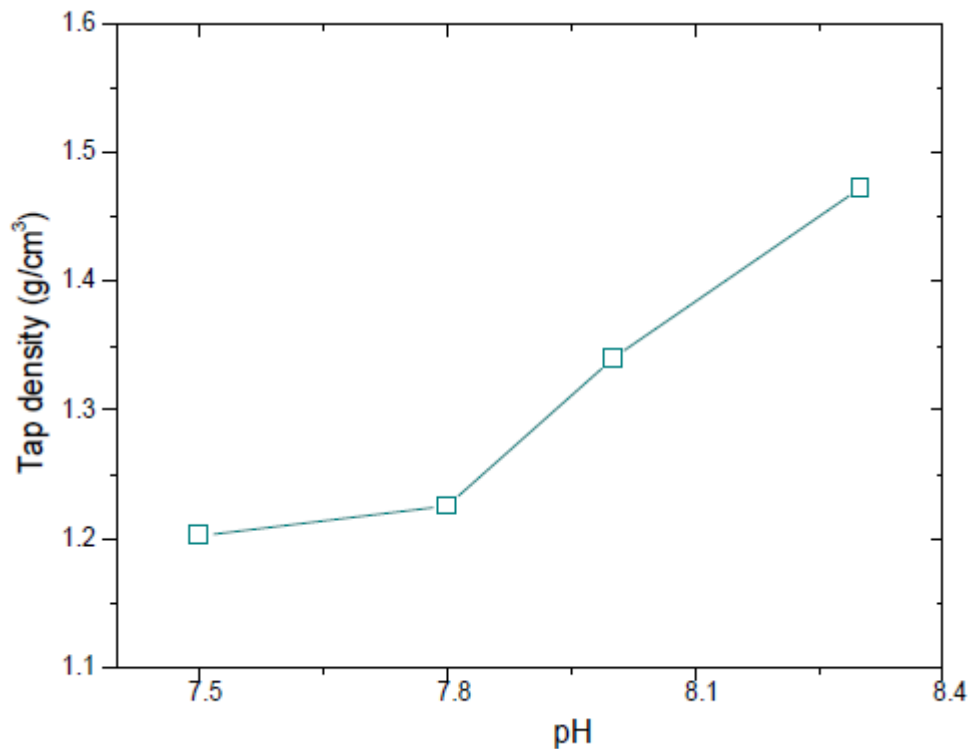


Figure 7. Tap density of $\text{Ni}_{0.5}\text{Mn}_{1.5}(\text{CO}_3)_2$ as a function of the preparation pH. Maximum value was obtained for a preparation pH of 8.3.

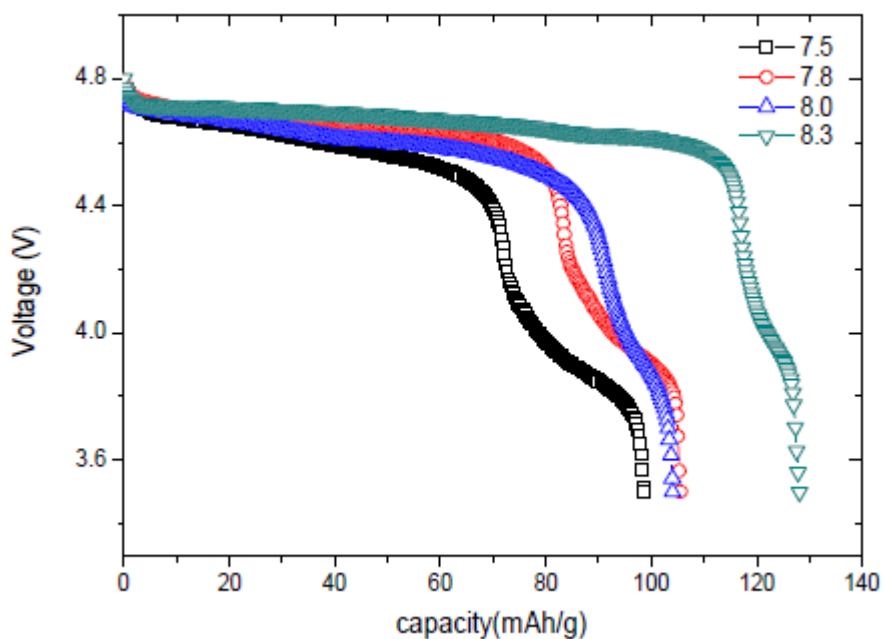


Figure 8. Charge/discharge curves for the $\text{LiNi}_{0.5}\text{Mn}_{1.5}\text{O}_4$ synthesized by co-precipitation at different preparation pH values. Sample synthesized at a preparation pH of 8.3 had the highest capacity.

The specific capacity for 4.7V for preparation pH values of 8 is larger than the sample for preparation pH values of 7.8. A summary of the electrochemical results is provided in Fig. 9 for the respective cycle lives.

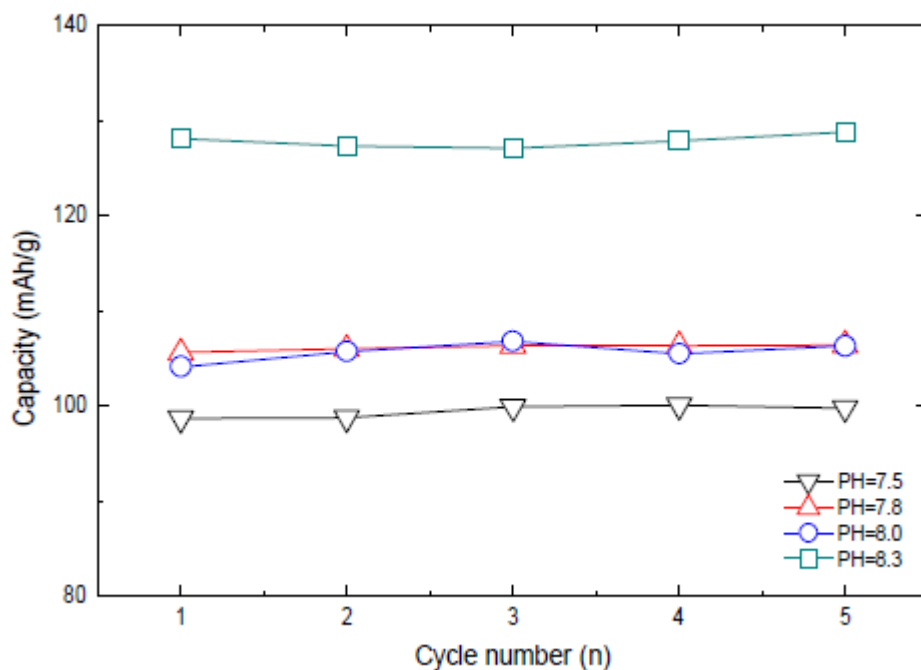


Figure 9. Cycling performance of $\text{LiNi}_{0.5}\text{Mn}_{1.5}\text{O}_4$ synthesized at different pH values.

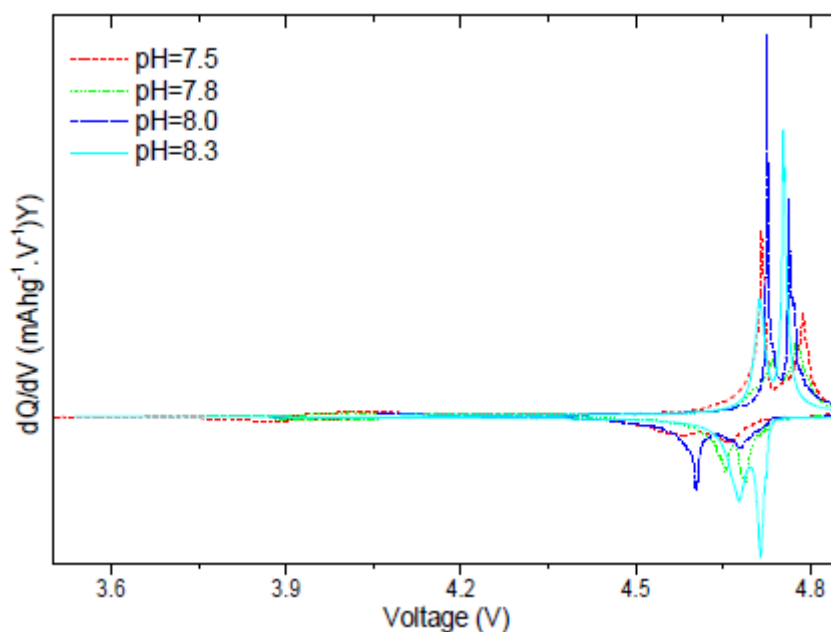


Figure 10. Differential capacity vs voltage curves for the $\text{Li}/\text{LiNi}_{0.5}\text{Mn}_{1.5}\text{O}_4$ cells between 3.5 and 4.9 V.

Fig. 10 shows dQ/dV curves for Li/LiNi_{0.5}Mn_{1.5}O₄ cells between 3.5 and 4.9 V. The dQ/dV curves indicate that all samples have two oxidation peaks with corresponding reduction peaks.

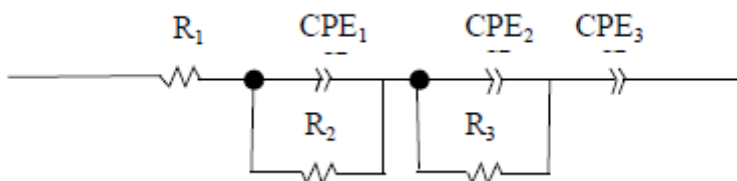


Figure 11. The equivalent circuit for spinel LiNi_{0.5}Mn_{1.5}O₄.

EIS is a fast and nondestructive detection technique that is frequently applied to the study of LNMS cathodes in lithium batteries [10-12]. The equivalent circuit shown in Fig. 11 was used to fit the EIS data. Fig. 12 also shows impedance spectra of the LiNi_{0.5}Mn_{1.5}O₄ electrode. The first frequency arc comes from Li⁺ migration through the interface between the surface layer of the material particles and the electrolyte, and the second low-frequency arc comes from the charge transfer process [13-15]. In this equivalent circuit, R₁ represents the ohmic resistance while R₂ and R₃ are the resistances of the SEI film and the charge transfer reactions, respectively, and CPE₁ and CPE₂ represent the capacitance of the SEI film and the capacitance of the double layer, respectively. CPE₃ is used to replace finite diffusion.

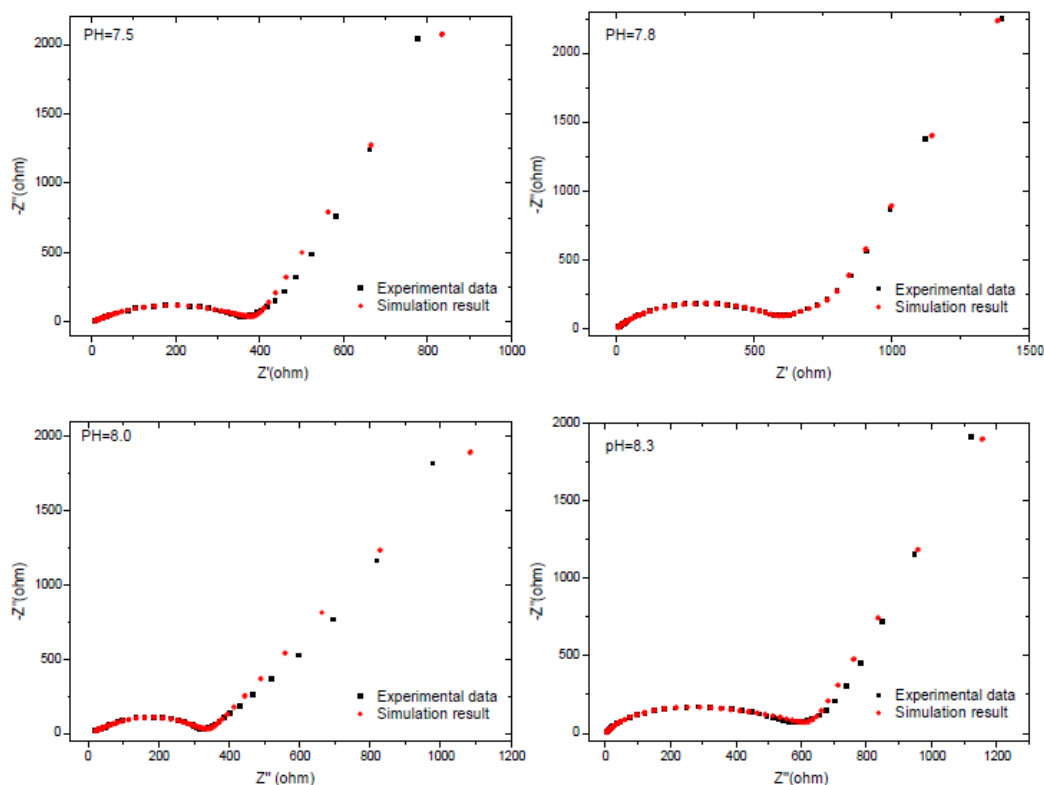


Figure 12. Equivalent circuit proposed for the EIS of spinel LiNi_{0.5}Mn_{1.5}O₄ and simulation results.

As shown in Fig. 12, the proposed model describes the experimental data very well. From the electrochemical impedance spectrum the diffusivity of the Li⁺ ions can be obtained according to the following equation [16]:

$$D = R^2 T^2 / 2 A^2 n^4 F^4 C^2 \sigma^2$$

where R is the gas constant, T is the absolute temperature, n is the number of electrons transferred per molecule during oxidation, F is the Faraday constant, A is the surface area of the electrode, C is the concentration of Li ions and σ is the Warburg factor, which is related to Z':

$$Z' = R_e + R_{ct} + \sigma \omega^{-1/2}$$

here, ω is the angular frequency in the low-frequency region.

The Li⁺ ion diffusion coefficients are also shown in Table 2. The material synthesized at a pH of 8.3 had the highest Li ion diffusion coefficient of 1.1735e⁻¹⁵ cm²/s.

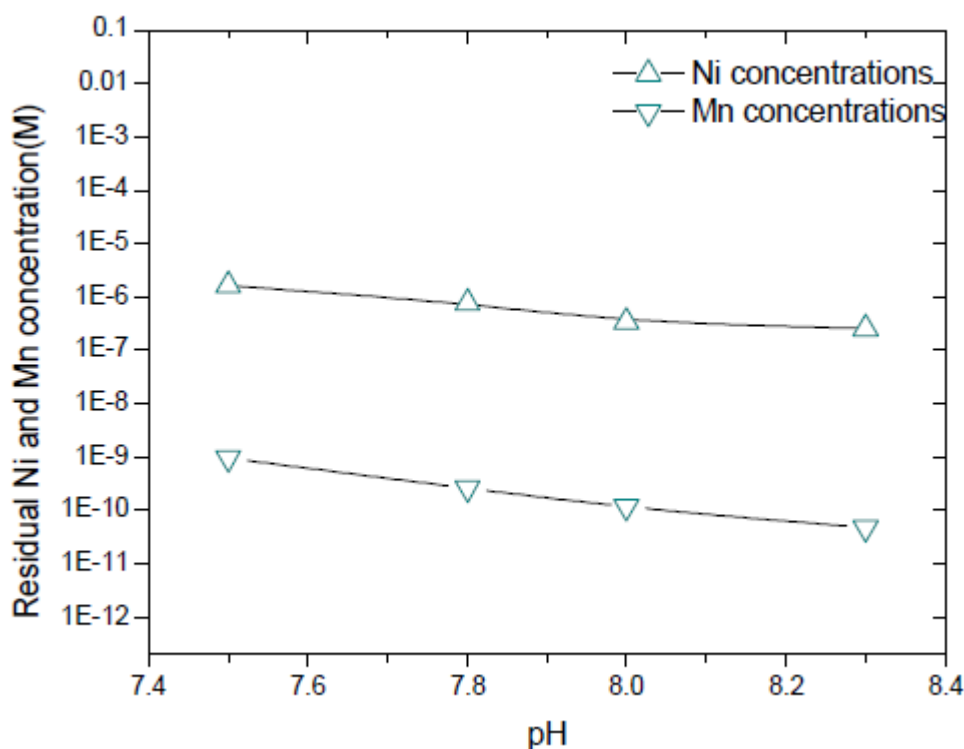


Figure 13. Residual Ni²⁺ and Mn²⁺ concentrations as a function of preparation pH.

Table 2. Diffusivity of the Li ions and parameters obtained from the simulation of elements in the equivalent circuit.

Samples	pH=7.5	pH=7.8	pH=8.0	pH=8.3
D _{Li+} (cm ² /s)	1.0960e-16	4.6919e-16	5.8344e-16	1.1735e-15

4. DISCUSSION

Lithium nickel oxide has not been pursued in its pure state as a battery cathode for various reasons. Most reports suggest that excess nickel is present in $\text{Li}_{1-y}\text{Ni}_{1+y}\text{O}_2$ [17]. The actual ionic distribution of LiNiO_2 can be represented as $[\text{Li}_{1-\delta-\omega}\text{Ni}_{\delta+\omega}^{2+}]_{3b}[\text{Ni}_{1-\delta}^{2+}\text{Ni}_{\delta-\omega}^{3+}\text{Li}_{\omega}]_{3a}\text{O}_2$ because of the presence of Ni ions in the Li layer [18]. Kim et al. reported a high Ni content of 5.9% in Li sites for samples of $\text{LiNi}_{1/3}\text{Mn}_{1/3}\text{Co}_{1/3}\text{O}_2$ that were prepared at 950 °C [19]. The layered oxide structure has lithium ions at the 3a sites, transition metal ions (Ni, Co, Mn) at the 3b sites and oxygen ions at the 6c sites. Since the ionic radii of the Li^+ (0.76 Å) and Ni^{2+} (0.69 Å) ions are similar, a partial disordering among the 3a and 3b sites is expected and is referred to as cation mixing [20]. A partial disordering of Li^+ and Ni^{2+} among the 8a and 16d sites occurs in $\text{LiMn}_{1.5}\text{Ni}_{0.5}\text{O}_4$.

The residual Ni^{2+} and Mn^{2+} concentrations was affected by pH [1]. According to the calculation method, the residual Ni^{2+} and Mn^{2+} concentrations decreased with an increase in preparation pH [21]. Fig. 13 shows the calculated residual Ni^{2+} and Mn^{2+} concentrations as a function of pH. The residual Ni^{2+} and Mn^{2+} concentrations decreased with an increase in preparation pH. A relationship exists between the residual Ni^{2+} and Mn^{2+} concentrations and the occupation of Ni^{2+} ions in the lithium site in preparation pH from 7.5 to 8.3.

5. CONCLUSION

Ni substitution occurred at the Li site in the $\text{LiNi}_{0.5}\text{Mn}_{1.5}\text{O}_4$ compounds prepared at pH values of 7.5, 7.8, 8.0 and 8.3. With an increase in preparation pH, the amount of Ni substitution at the Li site decreased. The analysis indicated that a relationship exists between the residual Ni^{2+} and Mn^{2+} concentrations and the occupation of Ni^{2+} ions in the lithium site in preparation pH from 7.5 to 8.3. With the lowest the Ni substitution occurring at the Li site at pH values of 8.3, $\text{LiNi}_{0.5}\text{Mn}_{1.5}\text{O}_4$ has the highest specific discharge capacity.

ACKNOWLEDGEMENTS

This work was financially supported by National Natural Science Foundation of China (Grant No.51202131), Qingdao development progress project (Grant No. 12-1-4-6-(11)-jch) and Shandong Province Natural Science Foundation (Grant No. ZR2012EMQ002).

References

1. D. P. Wang, I. Belharouak, G. M. K, Jr, G. W. Zhou and K. Amine, *Journal of Materials Chemistry*, 21 (2011) 9290.
2. K. Amine and J. Liu, *ITE Lett*, 1 (2000) 59.
3. K. Amine, C. H. Chen, J. Liu, M. Hammond, A. Jansen, D. Dees, I. Bloom, D. Vissers and G. Henriksen, *Journal of Power Sources*, 97 (2001) 684.
4. R. Santhanam and B. Rambabu, *Journal of Power Sources*, 195 (2010) 5442.
5. Z. S. Wronski, *International Materials Reviews*, 46 (2001) 1.
6. Y. Xia, Y. Zhou, M. Yoshio, *Journal of the Electrochemical Society*, 144 (1997) 2593.

7. T. Ohzuku, S. Takeda and M. Iwanaga, *Journal of Power Sources*, 81 (1999) 90.
8. A. V. Bommel and J. R. Dahn. *Chemical Materials*, 21 (2009) 1500.
9. S.B.Park, W.S.Eom, W. I.Cho, H. Jang, *Journal of Power Sources* 159 (2006) 679 .
10. M. Boris, T. Yosef, S. Gregory, A. Dorom, K. H. Jin and C. Seungdum, *Electrochemistry Communications*. 6 (2004) 821.
11. R. Dedryvere, D. Foix, S. Franger, S. Patoux, L. Daniel and D. Gonbeau. *The Journal of Physical Chemistry C*. 114 (2010) 10999.
12. J. Liu and A. Manthiram, *Journal of the Electrochemical Society*, 156 (2009) A66
13. N. M. Hagh, F. Cosandey, S. Rangan, R. Bartynski and G. G. Amatucci. *Journal of the Electrochemical Society*, 157 (2010) A305.
14. Y. Ding, P. Zhang and Y. Jiang, *Materials Research Bulletin*, 43 (2008) 2005.
15. X. Li, Y. J. Wei, H. Ehrenberg, F. Du, C. Z. Wang and G. Chen, *Solid State Ionics*, 178 (2008) 1969.
16. P. P. Prosini, M. Lisi, D. Zane and M. Pasquali, *Solid State Ionics*, 148 (2002) 45.
17. J. M. Tarascon, W. R. McKinnon, F. Coowar, T. N. Bowmer, G. Amatucci and D. Guyomard, *J. Electrochem. Soc.*, 141 (1994) 1421.
18. C. Poullierie and E. Suard, C. Delmas, *Solid State Chemistry*, 158 (2001) 187.
19. J. M. Kim and H. T. Chung, *Electrochimica Acta.*, 49 (2004) 937.
20. Z. Chen and J. R. Dahn, *Electrochemical and solid-state letters*, 5 (2002) A213.
21. J.T.Su, Y.C.Su, Z.G.Lai, P.Yu and X.D.He, *Journal of the chinese ceramic society*, 34(2006)695.

© 2014 The Authors. Published by ESG (www.electrochemsci.org). This article is an open access article distributed under the terms and conditions of the Creative Commons Attribution license (<http://creativecommons.org/licenses/by/4.0/>).